Hindawi Publishing Corporation
International Journal of Distributed Sensor Networks
Volume 2014, Article ID 709135, 10 pages
http://dx.doi.org/10.1155/2014/709135

Research Article

Energy Consumption Optimisation for Duty-Cycled Schemes in Shadowed Environments

Tatjana Predojev,[1] Jesus Alonso-Zarate,[1] Mischa Dohler,[2] and Luis Alonso[3]

[1] *Centre Tecnològic de Telecomunicacions de Catalunya (CTTC), Parc Mediterrani de la Tecnologia, Building B4, Avenida Carl Friedrich Gauss 7, Castelldefels, 08860 Barcelona, Spain*
[2] *Department of Informatics, King's College London, Strand, London WC2R 2LS, UK*
[3] *Universitat Politècnica de Catalunya, Parc Mediterrani de la Tecnologia (PMT), Esteve Terrades 1, Castelldefels, 08860 Barcelona, Spain*

Correspondence should be addressed to Tatjana Predojev; tatjana.predojev@cttc.es

Received 31 December 2013; Accepted 14 May 2014; Published 28 May 2014

Academic Editor: Sana Ullah

The focus of this study is the optimal configuration of a wireless low-power duty-cycled network with respect to the minimal energy consumption. Precisely, the energy consumption of a truncated-ARQ scheme in realistic shadowing environments is examined for the reference IEEE 802.15.4e standard protocol and for its cooperative extension that is presented in the paper. We show how to choose between the direct or multihop forwarding and the cooperative version of the two. We determine the optimal forwarding strategy for both loose and strict reliability requirements. Low-power links are parametrised by the interdevice distance and the corresponding outage probability, for the fixed output transmission power. It is shown that significant amounts of energy can be saved when the most adequate scheme of the three is applied. All analytical results are validated in the network simulator ns-3.

1. Introduction

A device domain of the machine-to-machine (M2M) communication system largely consists of resource-constrained, low-power, and energy-efficient devices. Following years of research and fine-tuning, viable technical solutions for achieving the adequate low energy regime have been devised and the standardised protocol stack has been put forward [1]. The lifetime of wireless M2M devices is measured in years or decades; extreme energy efficiency is thus a must and only achieved through aggressive duty-cycling [2]. A duty-cycled device keeps the radio transceiver in sleep state most of the time, except for the periodic wake-ups used to transmit the collected data. In this way, both overhearing and idle listening are evaded with the goal of conserving energy. The IEEE 802.15.4e standard amendments [3] define the required duty-cycled scheme. Arguments for applying this scheme are provided in [1] that examines the most energy-efficient solutions over the entire protocol stack. With the standardised protocol stack in place, remaining work is to find the adequate device configuration which includes the optimal forwarding strategy, in realistic environments. These issues are addressed in our study.

Link (un)reliability is core to our study: it is known that short interdevice distances typically imply more reliable links, whilst reliability decreases with the increase in distance. Therefore, one of the key parameters in our work is the optimal interdevice distance under the typical (low) values of output transmission power. We characterise the resulting link (un)reliability with the link outage probability. Link outages result in discarded packets; therefore, outage probability provides the estimation of link quality. In addition, this approach enables network design under outage constraints specified in advance.

In order to formulate the energy consumption model for the protocol stack of M2M low-power devices, we start by deducing a link metric that considers realistic operating conditions. Physical layer studies (e.g., [4]) typically focus on the physical phenomena of the wireless channel and related effects on the error probability. The channel is thus subject

to large-, medium-, and/or small-scale fading, with the latter two in time being static, block, or fast. On the other hand, the studies of upper layers experimentally measure the impact of wireless channel, such that the channel effects are reflected in bursty or independent link behaviour (e.g., [5]). We connect the two approaches into the link layer analytical model, while capitalising on the results and observations of previous works. Indeed, we analyse how wireless channel effects interact with higher layers, link layer in particular, and how this interaction affects the link quality. A metric we propose is dependent on two critical parameters under study: link distance and the related outage probability. This metric is the Average Number of Transmissions per Packet $\overline{N}_{tx}$. By considering outages at the link layer, we provide original approach in the analysis of low-power, unreliable links.

Accurate link characterisation offers insight into how to optimise the overall energy consumption. For example, dynamic forwarding is an effective way of combating link outages through path diversity. Using other available links when primary link is in outage eventually saves energy. Specifically, we focus on the Cooperative Automatic Repeat reQuest (C-ARQ) as a reactive form of dynamic forwarding. Traditionally, C-ARQ relies on overheard packets by the neighbouring devices which then become relays [6]. In a duty-cycled scheme, this is not possible. Therefore, we specifically adapt the C-ARQ technique to the duty-cycled scheme without assuming overhearing at the relay and optimise it for the most energy-efficient operating regime. The resulting scheme is denoted as Cooperative and Duty-Cycled ARQ (CDC-ARQ). The main idea of our CDC-ARQ scheme is to introduce path diversity in the scheduling functions. Opposed to C-ARQ, CDC-ARQ does not rely on overhearing, but rather on the analysis of wireless low-power links. We consider realistic wireless channel with shadow fading. In the analysis, we focus on the specifics of low-power M2M networks in order to present customised results that are ready applicable in practice. Nevertheless, our analytical model supports changes in the modulation or coding scheme, output transmission power, and so forth. One of the key features of CDC-ARQ technique is that it can be easily fitted into the standard, as no changes must be done to the physical (PHY) nor the medium access control (MAC) layers but just to the scheduling functions. All references to the standard in the paper refer to IEEE 802.15.4e [3].

Previously, we developed this idea in [7, 8]. In [7], the star topology is examined and it is shown that benefits can be obtained by forwarding through a relay after the initial transmission failure. In [8], we establish a cooperative communication scheme applicable to any topology and evaluate the scheme's energy consumption. In the present paper, we extend the analysis beyond cooperative scenario to offer a comprehensive overview of low-power wireless links. For a given outage probability constraint, we find the most energy-efficient forwarding strategy of the three available choices: direct, multihop, or CDC-ARQ forwarding. CDC-ARQ for a duty-cycled device alternates between the direct and multihop forwarding depending on the channel conditions.

In summary, the main contributions of this paper are as follows.

(1) A link energy consumption model is formulated to reflect the wireless channel effects.

(2) Link selection guidelines are provided which strive to minimise the overall energy consumption, for either loose or strict reliability requirements. In particular, the bounds for the efficient direct, multihop, or CDC-ARQ forwarding are derived and presented.

Finally, the analytical model provided in this paper is validated in ns-3 network simulator [9]. An ns-3 simulation mimics the real world as close as possible, since the implementation closely follows the related standard technology. Therefore, aside from validating our analytical model, we show that the techniques presented here are suitable for real devices and can be easily integrated into IEEE 802.15.4e standard.

The remainder of the paper is organised as follows: Section 2 lists some related works. Section 3 presents the system model. Section 4 contains the derived analytical energy model. The model validation is presented in Section 5 together with the results extended beyond the model in the simulations. Finally, the paper is concluded in Section 6.

2. Related Work

The optimal link distance that maximises energy efficiency has been previously investigated in [10] for different node densities and path loss exponents. The results obtained in [10] apply to a circular coverage area without considering the fading effects, which are acknowledged in this work. With the distance fixed, various cooperative schemes have been put forward in the literature in order to improve the reliability without trading it for higher energy consumption. Vardhe et al. study cooperation using distributed space time codes in [11], for equidistant relays on a direct path to destination. In [12], the energy efficiency of direct, multihop, and cooperative transmission schemes is studied for fixed outage probability in order to find the optimal output transmission power; the results, however, span the range of output power values significantly above the typical setting for the M2M low-power networks. These works apply to nonduty-cycled schemes and thus assume overhearing as the basis for cooperation which makes them unsuitable for duty-cycled systems envisioned in [3].

To overcome the complexity of cooperative scheme implementation at the PHY layer (such as synchronisation issues), cooperation at the link layer presents an alternative in the form of C-ARQ. In a C-ARQ scheme, a device seeks cooperation from neighbours to reroute data packets locally in the case of a temporary wireless channel outage on the primary link. C-ARQ for nonduty-cycled schemes was analytically studied in [13]. Alizai et al. take an experimental approach in [14] to show that a rerouting technique decreases the total number of packet (re)transmissions in low-power networks. A detailed energy consumption analysis is still needed to quantify the actual benefits and, therefore, configure

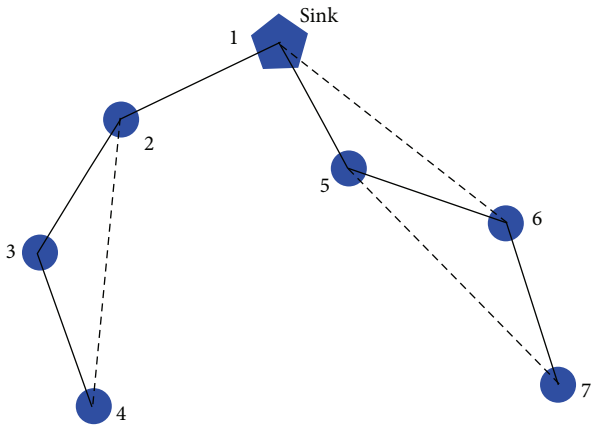

Figure 1: M2M device network scenario; solid line stands for a high-quality link and dashed line stands for a medium-quality link.

the links accordingly. Cooperation at the link layer is simpler to implement in duty-cycled systems compared to the more complex PHY cooperative schemes.

A cost metric similar to ours to characterise the link quality was previously investigated in [15]. However, in [15], indefinite packet retransmissions until success were assumed, which results in significant energy cost in outage conditions, thus diverging from the optimal solution. The cost metric in [15] was verified experimentally, while we take an analytical approach that is validated by comprehensive simulations. Authors in [16] study the problem of dynamic data forwarding depending on the link quality from the routing perspective. Based on the results, they conclude that the dynamic forwarding provides highly robust and reliable systems.

3. System Model

3.1. Scenario. An M2M device network is considered, consisting of N devices and a data collector denoted sink. A traffic pattern is convergecast towards the sink and the devices may opt for a direct or a multihop transmission to the sink if a direct link cannot be established. The number of hops on a multihop path is denoted as k. Any link that can improve progress to the sink by decreasing k is denoted as a direct link. To transmit a packet to the sink, various combinations of links between a pair of devices can be formed, as shown in Figure 1. The links represented with solid lines are short-range and on average more reliable than the medium-range links represented with dashed lines. Therefore, we classify a short-range link with small probability of error as a high-quality link, distinguished from a medium-range link with greater probability of error denoted as a medium-quality link. The unreliability that is bound to the medium-range links is the main reason why they are usually discarded, even though they offer better progress to the sink.

3.2. Medium Access Control Layer. We consider time synchronised channel hopping (TSCH) mode of the MAC protocol in IEEE 802.15.4e [3]. It defines a fixed time division multiple access (TDMA) frame structure that is centrally scheduled. Each *link* formed by a pair of neighbour devices is assigned to a unique time slot that repeats in a cyclical manner. The receiver wakes up only in the assigned slot and may enter a sleep state (i.e., switch off its radio transceiver) for the rest of time. After it has woken up, it either receives a packet if the transmitter has one to send or goes quickly back to sleep if a packet preamble is not detected within a short, predefined time interval, that is, a fraction of the slot duration. The slot without a packet transmission is denoted as the *idle listen* slot. We consider dedicated links that are scheduled for each transmitter-receiver pair to prevent packet collisions.

3.3. CDC-ARQ Overview. CDC-ARQ technique enables the efficient use of medium-range links. CDC-ARQ operates as follows: each new transmission is first attempted over the direct, medium-quality link, for example, over link 4-2 in Figure 1. If it fails, the packet is redirected to the multihop path that offers higher reliability (4-3-2). Time slots are assigned both for the medium-range and medium-quality links, as well as for the backup multihop path that consists of short-range equidistant links, as shown in Figure 2. If the initial attempt over medium-quality link succeeds, the receivers on backup links only perform idle listen in the fraction of their slots. With CDC-ARQ, two forwarding options cooperate to provide a better service for the current channel realisation. Short-range links are approximated to be equidistant and k times shorter than the direct links. The goal is to find a link distance coupled with the appropriate forwarding scheme that results in minimum energy consumption.

3.4. Modulation and Coding. To exemplify the analysis, we focus on the transceiver of the IEEE 802.15.4 radios, working in the 2.4 GHz band, whose bit error rate p_b is given by [17]

$$p_b(\gamma) = \frac{8}{15} \cdot \frac{1}{16} \cdot \sum_{i=2}^{16} -1^i \binom{16}{i} e^{(20\gamma(1/i-1))}, \quad (1)$$

where γ is the instantaneous signal-to-noise-ratio (SNR) at the receiver. The packet success probability p_s assuming independent bit errors is

$$p_s(\gamma) = (1 - p_b)^L, \quad (2)$$

where L is the packet size in bits. The packet error probability p_e is therefore $p_e = 1 - p_s$. Note that p_s depends on the instantaneous γ characterized by the channel dynamics.

3.5. Channel Model. The wireless signal strength decays exponentially with distance as described by the *large-scale* pathloss channel model. Superimposed on this deterministic value is the random *medium-scale* fading model (also known as *shadowing*) and *small-scale* multipath fading. Given the transmission power P_t, the mean power at the receiver P_r is therefore

$$P_r(\text{dBm}) = P_t(\text{dBm}) - \text{PL}(d_0) - 10\alpha \log_{10} d - X_\sigma, \quad (3)$$

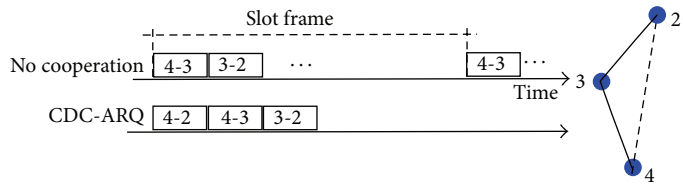

Figure 2: TDMA slot scheduling with and without cooperation.

where $\mathrm{PL}(d_0)$ is the pathloss at reference distance d_0, α is the pathloss exponent, d is the link distance from the transmitter, and $X_\sigma \sim N(0,\sigma)$ is a normal random variable (on dB scale). On a linear scale, normal distribution becomes lognormal such that X_σ models the random component of a wireless signal. Given the average receiver thermal noise P_n in dBm, the mean SNR at the receiver (when fading effects are averaged out) is $\mu(\mathrm{dB}) = P_r - P_n$. Recall that the instantaneous SNR at the receiver that varies in space and time is denoted as γ. For a given μ, the instantaneous γ expressed on a linear scale is lognormally distributed and conditioned on μ and with standard deviation σ, both expressed in dBs, the probability density function (pdf) of which is

$$p_\gamma(\gamma \mid \mu) = \frac{10}{\ln 10\sqrt{2\pi}\sigma\gamma} \exp\left[-\frac{(10\log_{10}\gamma - \mu)^2}{2\sigma^2}\right]. \quad (4)$$

We assume that channel hopping in the TSCH scheme alleviates small-scale multipath fading for packet retransmissions. The shadowing effect resulting from large moving obstacles remains. Similar channel model with lognormal shadowing was adopted in [18], but static environment was assumed where γ remains constant for long time intervals.

In dynamic environments, the assumption of γ being constant in time no longer holds. The empirical study of low-power wireless links in [5] showed that γ is correlated in time on scales larger than a packet duration, which results in effect denoted as link *burstiness*. In addition, medium success rate on a link is not the result of a corresponding constant packet success probability $p_s(\gamma)$, but rather the consequence of frequent oscillations between the nearly perfect and outage states that, when averaged, result in a medium-quality link. Based on these empirical observations, that are revisited and confirmed in [19], and essentially adopting a block-fading channel, we make the following assumptions:

(i) the realization of the channel fading, both comprising small-scale fading and shadowing, is drawn from distribution in (4);

(ii) the system is duty-cycled such that for every original packet a new realization of γ according to lognormal distribution is encountered;

(iii) in case of a transmission error, the packet is retransmitted up to $N_{\max}$ number of attempts (truncated-ARQ) where each retransmission encounters again the same value of γ on the same link.

The last assumption is based on the fact that packet retransmissions are sufficiently close in time to experience link burstiness described in [5]. New packets however are generated at a rate at which burstiness effect disappears. Therefore, independent channel realisation is assumed for new packets.

3.6. Energy Model. From the exemplary radio transceiver data sheets, for example, [20], we distinguish two basic radio power modes (voltage $V_{DD} = 3\,\mathrm{V}$), with the associated current consumption:

(1) *sleep*, $I_s \approx 0$,

(2) *awake* (also, *on*), that further exhibits two submodes:

(i) *active*, either transmitting or actively receiving $I_{tx} \approx I_{rx} = I_a = 20\,\mathrm{mA}$,

(ii) *idle* (*listen*), waiting for signal $I_{\mathrm{id}} = 2\,\mathrm{mA}$.

We assume that the output transmission power is set to $P_t = 0\,\mathrm{dBm}$. The energy is calculated as the product of the power consumption of a mode and the time spent in that power mode (power $P_x = V_{DD} \cdot I_x$, energy $E_x = P_x \cdot T$, where x can stand for sleep s, transmitting tx, actively receiving rx, or idle listen id). Power modes change within a slot according to TSCH algorithm. Before a transmission, clear channel assessment (CCA) is performed. There is no random backoff and no contention (recall that slots are dedicated). CCA is introduced for coexistence with other systems (e.g., IEEE 802.11 network) with whom the same physical space is shared. Therefore, a device performing CCA in TSCH mode listens to the wireless channel for a fixed time interval to determine whether it is free. If yes, a packet transmission follows; if not, a transmission is delayed until the next slot. An idle radio power mode is activated when there is no data transmission resulting in the idle listen slot of duration T_{id}, if a device is performing clear channel assessment for the time duration T_{cca} and between the end of data transmission and before the beginning of acknowledgement (ACK) for T_{ad} (ACK delay). Since the energy consumption in the sleep state can be neglected, we do not include it in our model. To calculate the time duration of active power modes, packet lengths (in bits) are divided with the data bit rate, $T_{\mathrm{data}} = L/R_b$ and $T_{\mathrm{ack}} = L_{\mathrm{ack}}/R_b$. Finally, we can define three basic energy consumption components associated with the MAC layer described in Section 3.2:

$$\begin{aligned} E_{\mathrm{data}} &= T_{\mathrm{cca}} \cdot P_{\mathrm{id}} + T_{\mathrm{data}} \cdot (P_{tx} + P_{rx}), \\ E_{\mathrm{ack}} &= T_{ad} \cdot P_{\mathrm{id}} + T_{\mathrm{ack}} \cdot (P_{tx} + P_{rx}), \\ E_{\mathrm{idle}} &= T_{\mathrm{id}} \cdot P_{\mathrm{id}}. \end{aligned} \quad (5)$$

Note that the energy components include the energy spent both at a transmitter and at a receiver.

4. Energy Analysis for Low-Power Links

4.1. Average Number of Transmissions per Packet. If the upper bound on the allowed number of transmission attempts per packet $N_{\max}$ was not set, huge amounts of energy would be wasted in periods of channel outage because the packet would be continuously retransmitted without success until the channel became available again. This is why the truncated-ARQ is applied to discard a packet if it was transmitted $N_{\max}$ times and still not successfully delivered. While truncated-ARQ can save significant amounts of energy, it produces a certain packet loss on a link that can be measured with the outage probability parameter.

Taking the channel model described in Section 3.5, the average number of transmissions for one realization of γ is then

$$\begin{aligned} N_{tx}(\gamma) = {} & 1 \cdot (1 - p_e(\gamma)) + 2 \cdot p_e(\gamma)(1 - p_e(\gamma)) \\ & + 3 \cdot p_e(\gamma)^2 (1 - p_e(\gamma)) + \cdots \\ & + N_{\max} p_e(\gamma)^{N_{\max}-1} (1 - p_e(\gamma)) \\ & + N_{\max} p_e(\gamma)^{N_{\max}}. \end{aligned} \tag{6}$$

Recall that γ remains constant for all retransmissions. The last member of the sum denotes the packets that were received erroneously $N_{\max}$ times and discarded. After some simple algebra we get

$$N_{tx}(\gamma) = \sum_{n=1}^{N_{\max}} p_e(\gamma)^{n-1} = \sum_{n=1}^{N_{\max}} (1 - p_s(\gamma))^{n-1}. \tag{7}$$

The average number of transmission attempts per packet, over all γ realization, is then

$$\overline{N}_{tx}(\mu) = \int_0^{\infty} N_{tx}(\gamma)\, p_\gamma(\gamma \mid \mu)\, d\gamma. \tag{8}$$

Note that because the integrand in (7) is applied instead of $p_s(\gamma)$ (the latter is usually studied), γ is kept constant for all the retransmissions to reflect the empirically observed link temporal correlation. No approximation for high SNR values can be applied since the lower limit of integration is zero. Therefore we solve the integral in (8) numerically.

4.2. Outage Probability. We define the outage probability p_{out} as the probability that a packet is discarded after $N_{\max}$ failed transmission attempts. To calculate p_{out}, we use the average number of errors associated to a realization of γ as follows:

$$\begin{aligned} N_{\text{err}}(\gamma) &= \sum_{n=0}^{\infty} n \cdot (p_e(\gamma))^n \cdot (1 - p_e(\gamma)) \\ &= \frac{p_e(\gamma)}{1 - p_e(\gamma)}. \end{aligned} \tag{9}$$

A link is in outage if the current value of γ is such that the associated average number of errors is $N_{\text{err}} \geq N_{\max}$. Taking the inverse function of (9), we can find the threshold γ_{th} such that $\gamma_{\text{th}} = N_{\text{err}}^{-1}(N_{\max})$. Therefore, if the current realization of γ satisfies $\gamma \leq \gamma_{\text{th}}$, the link is said to be in outage. If γ is lognormally distributed, there is a nonzero outage probability for every device involved in communication regardless of the value of μ. The outage probability can be computed as [4]

$$\begin{aligned} p_{\text{out}} &= \int_0^{\gamma_{\text{th}}} p_\gamma(\gamma \mid \mu)\, d\gamma \\ &= Q\left(\frac{\mu - 10 \log_{10}(\gamma_{\text{th}}(N_{\max}))}{\sigma} \right), \end{aligned} \tag{10}$$

where $Q(\cdot)$ is the tail integral of a unit Gaussian probability density function.

4.3. Energy Consumption Analysis. The mean energy spent both at the transmitter and at the receiver to exchange a packet over a link, that is, per time slot, is

$$\begin{aligned} E_{\text{link}} = {} & \overline{N}_{tx} \cdot E_{\text{data}} + (1 - p_{\text{out}}) \cdot E_{\text{ack}} \\ & + (N_{\max} - \overline{N}_{tx}) \cdot E_{\text{idle}}, \end{aligned} \tag{11}$$

where $\overline{N}_{tx}$ and p_{out} are defined in (8) and (10), respectively, and the energy components are defined in (5). In order to avoid buffering packets coming from the upper layer in the transmit queue, possible retransmissions need to be considered when the time frame is designed. Therefore some slots result in idle slots when there are no retransmissions and they are represented by the last component in (11). Both $\overline{N}_{tx}$ and p_{out} depend on the mean SNR μ whose relation to the link distance can be derived from (3).

For a fixed distance to the destination, a device may opt for a direct, multihop, or CDC-ARQ transmission. In case of a multihop transmission, we refer to the multihop path made of consecutive, equidistant links. A path begins with the source device, continues over $k - 1$ relays, and finally ends at the destination. The total mean energy spent to transmit a packet over a multihop path is

$$E_{\text{tot}} = \sum_{n=0}^{k-1} (1 - p_{\text{out}})^k \cdot E_{\text{link}}, \tag{12}$$

because only those packets that were delivered to a relay are forwarded over the next link and p_{out} is the outage probability of each individual link. For a direct transmission when $k = 1$, (12) gives $E_{\text{tot}} = E_{\text{link}}$. However, to single out the efficient part of the total consumed energy, we are interested in the energy spent per *delivered* packet, because if the packet does not reach the destination, the energy spent in a transmission attempt is wasted. The unit of effective energy consumption is thus *Joule per delivered packet*. The probability of discarding a packet on a multihop path is

$$p_{\text{out}}^t = 1 - (1 - p_{\text{out}})^k. \tag{13}$$

Therefore, we calculate the effective mean energy per delivered packet on a multihop path as follows:

$$E_{\text{eff}} = \frac{E_{\text{tot}}}{1 - p_{\text{out}}^{t}}. \tag{14}$$

In a direct transmission when $k = 1$, $E_{\text{eff}} = E_{\text{link}}/(1 - p_{\text{out}})$.

Finally, CDC-ARQ represents a combination of the two, as it alternates between the medium-range link and the multihop transmission depending on channel conditions. Recall that a transmission is first attempted over a direct link. If it results in error, the packet is immediately redirected because the probability of error for the subsequent attempts on the same link is high. If however the attempt over the direct link results in success, the time slots on a backup path remain idle. Therefore, the mean energy spent in a CDC-ARQ scheme for $k = 2$ backup multihop path is

$$E_{\text{carq}} = p_{\text{out}}^{c} \cdot \left(E_{\text{data}} + E_{\text{tot}}\left(k = 2\right)\right) + \left(1 - p_{\text{out}}^{c}\right) \cdot \left(E_{\text{data}} + E_{\text{ack}} + kN_{\max}E_{\text{idle}} + \left(N_{\max} - 1\right)E_{\text{idle}}\right), \tag{15}$$

where p_{out}^{c} is the probability of redirecting to a multihop path because of a direct link outage. The probability p_{out}^{c} corresponds to $N_{\text{err}} = 1$ (error on a direct link) and can be calculated from (10) for the given link distance by replacing $\gamma_{\text{th}} = N_{\text{err}}^{-1}(1)$. When the packet is redirected, we need to include the energy spent for the initial attempt that resulted in error. Otherwise, only the energy of the successful transmission with ACK is consumed plus the idle slots on a backup path. The effective mean energy per delivered packet is then

$$E_{\text{eff}}^{c}\left(k = 2\right) = \frac{E_{\text{carq}}}{1 - p_{\text{out}}^{c} \cdot p_{\text{out}}^{t}\left(k = 2\right)}, \tag{16}$$

where E_{eff}^{c} denotes the energy of the cooperative forwarding scheme as opposed to the energy of the fixed forwarding scheme E_{eff}.

Although the expressions for the network energy consumption in CDC-ARQ scheme for $k > 2$ are tractable, they can be quite complex because of multiple medium-range links that can be formed. That is why we chose to validate the model in the simulation with the simplest case of $k = 2$, which, in its turn, also validates the implementation in the simulator. Then we proceed with the evaluation in the simulator only for $k > 2$. This step is in line with the general tendency to validate the developed ns-3 code and thus support the trustworthiness of the simulation output. In addition, a quick access to complex scenarios justifies the use of a simulator.

For better readability, the notations used throughout the paper are summarized in notations section.

5. Performance Analysis

5.1. Implementation in ns-3 Simulator. ns-3 is an open-source, discrete-event network simulator written in C++. It consists of libraries for various technology models that implement the protocol interface and packet format (including the headers) by closely following the definitions of the corresponding standard. This approach enables a reliable simulation of the real system and facilitates the integration with a testbed. The final goal of a fully supported model is to enable each simulated device to run an entire protocol stack and generate the output trace that is (almost) indistinguishable from the output of a real device. Given that ns-3 is a network simulator, the unit of granularity is a packet, which contains both payload (in case of data packets) and a corresponding header. Each layer of a protocol stack executes its specified role; for example, the MAC layer at the transmitting side generates the MAC header, adds it to the payload received from the upper layer, and forwards a packet to the PHY layer where it is serialised and transmitted over the wireless channel as a set of bits.

The functionality required for this study has been implemented by modifying a model for the IEEE 802.15.4 standard, whose name is *lr-wpan* and whose source code can be downloaded from [21]. The MAC implementation available in the initial *lr-wpan* model supports the nonbeacon, mesh mode with all devices in the default idle listen state of the radio transceiver. This model has been significantly extended to include the duty-cycling operation of the devices, to support the energy consumption measurements, and to enable the path diversity necessary for the CDC-ARQ scheme. Firstly, duty-cycling has been implemented with TDMA as explained in Section 3.2. Contention during the CCA phase has been disabled and replaced with the simple CCA without random backoff as specified in [3]. Next, the existing log-distance path loss channel model has been extended with a realistic shadowing model described in Section 3.5 and defined with a standard deviation σ and a channel correlation in time. The CDC-ARQ functionality has been implemented by introducing dedicated tags in the packet header. Finally, the energy consumption module has been extended to subscribe to the changes in the state of a PHY radio transceiver in order to obtain the energy consumption directly from the device (i.e., from the simulated radio). The energy module is not aware of the wireless channel nor of the MAC layer scheme; therefore the two cannot interfere with the energy reading. Because of this design choice, an independent comparison with the theoretical model is provided.

5.2. Results

(1) Simulation Parameters. The default values of simulation parameters are given in Table 1. The maximum number of transmission attempts $N_{\max}$ is recommended in the standard, as well as the data bit rate that corresponds to the chosen frequency band; the modulation considered is offset quadrature phase-shift keying (O-QPSK) with additional direct sequence spread spectrum (DSSS), whose bit error rate is given in (1). The default header is generated in the simulation as specified in the standard [3].

(2) Link Metrics. The first step in the validation of the energy model is to show that the presented metrics, namely,

Table 1: Simulation parameters.

Parameter	Value
P_t	0 dBm
σ	4 dB
R_b	250 kbits/s
$N_{\max}$	4
L	27 bytes
freq. band	2.4 GHz

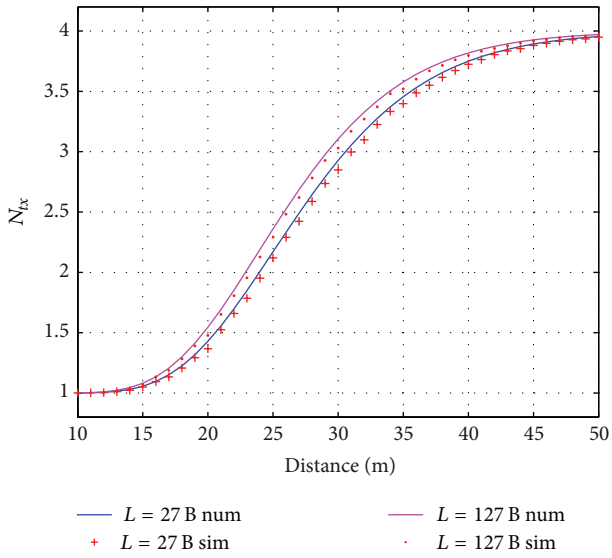

Figure 3: Average Number of Transmissions per Packet as a function of link distance; payload of minimum $L = 27$ bytes; and maximum length $L = 127$ bytes; truncated-ARQ, $N_{\max} = 4$.

$\overline{N}_{tx}$ paired with p_{out}, characterises a low-power wireless link reliably. To that aim, we observe a low-power link for various distances when the output transmission power P_t is fixed. Figure 3 shows the Average Number of Transmissions per Packet in a truncated-ARQ scheme over a low-power, shadowed wireless link. As the distance increases, more and more packets get discarded and $\overline{N}_{tx}$ approaches the maximum allowed number of attempts per packet. If the scheme was not truncated but indefinite retransmissions until successful delivery were permitted, in the considered shadowed environment the function $\overline{N}_{tx}$ would not be bounded. The unbounded function $\overline{N}_{tx}$ would tend to infinity which makes the analysis intractable. In general, system is designed such that outage states are brought to minimum because they destabilise the system. That is why the upper limit $N_{\max}$ had to be imposed on the number of transmission attempts. Not only does it limit the influence of outage states, but it also preserves energy and system resources, for the cost of some discarded packets. However, the probability of discarding a packet can be controlled either with careful system design or with CDC-ARQ. Figure 3 shows $\overline{N}_{tx}$ for the minimum and maximum packet lengths allowed by the standard (27 bytes $\leq L \leq$ 127 bytes). It can be seen that the packet size does not influence this metric significantly. The average number of

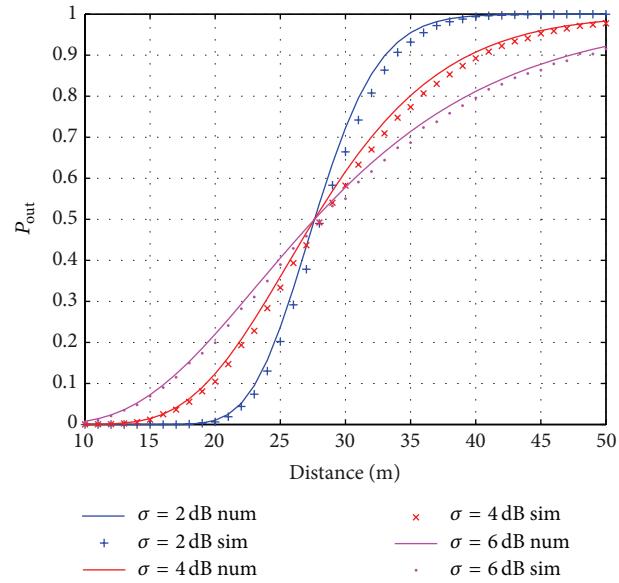

Figure 4: Outage probability as a function of link distance for different shadowing σ; output transmission power is set to 0 dBm.

transmissions is an important parameter in estimating the energy consumption since the energy is directly proportional to its value, as (11) shows. Note from Figure 3 that the results obtained in MATLAB for the numerical solution of (8) match well with the simulation results obtained in ns-3.

The (un)reliability of the scheme can be estimated with the number of packets that get discarded after $N_{\max}$ attempts. The outage probability p_{out} that complements the $\overline{N}_{tx}$ metric is shown in Figure 4 for several values of the standard deviation of shadowing σ. A value of the outage probability depicted in Figure 4 for a given link distance corresponds to a value of $\overline{N}_{tx}$ in Figure 3 for the same distance. For example, when $\overline{N}_{tx} = 2$ for $L = 27$ bytes, the $p_{\text{out}} = 0.3$ for $\sigma = 4$ dB; that is, 30% of packets are discarded on average over this link. With the increase in σ, the range of link distances with medium packet loss probabilities increases. In another words, without shadowing the graph would resemble the step function that produces the unrealistic circle coverage area with the perfect reliability within the circle and the absolute outage outside of it. The inclusion of shadowing effects makes every link unreliable, with the predictable (average) degree of unreliability p_{out}. The numerical estimation of p_{out} in (10) obtained in MATLAB agrees well with the number of discarded packets in ns-3 simulation. A slight disagreement is the consequence of the missed ACKs not considered in the theoretical model which cause retransmissions in the simulation. It has been determined by simulation that successfully delivered data packets whose ACK is not received do not exceed 5% of all the transmitted packets. The probability of unsuccessful ACK transmission approaches 5% for medium link outage probabilities, but it decreases to values below 2% for low or high outage probabilities. It can be seen in Figure 4 that the slight disagreement is highest precisely for the medium outage probabilities. In addition, observe that

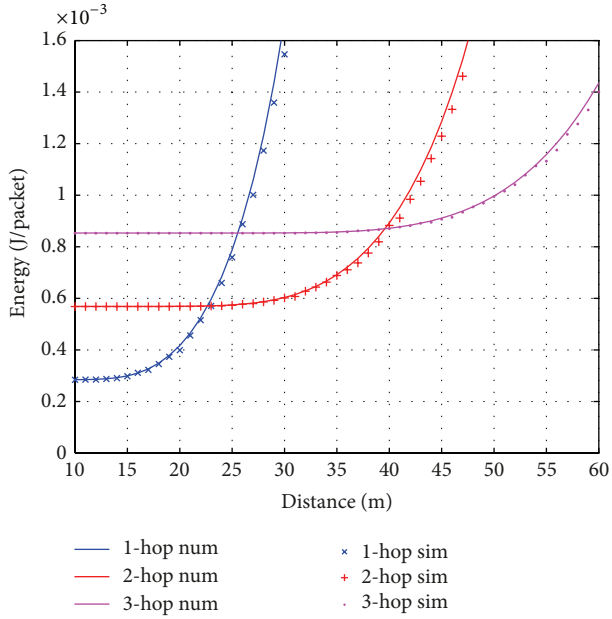

Figure 5: Total mean energy spent per delivered packet for direct, 2-hop, and 3-hop transmission over the total source-to-destination distance.

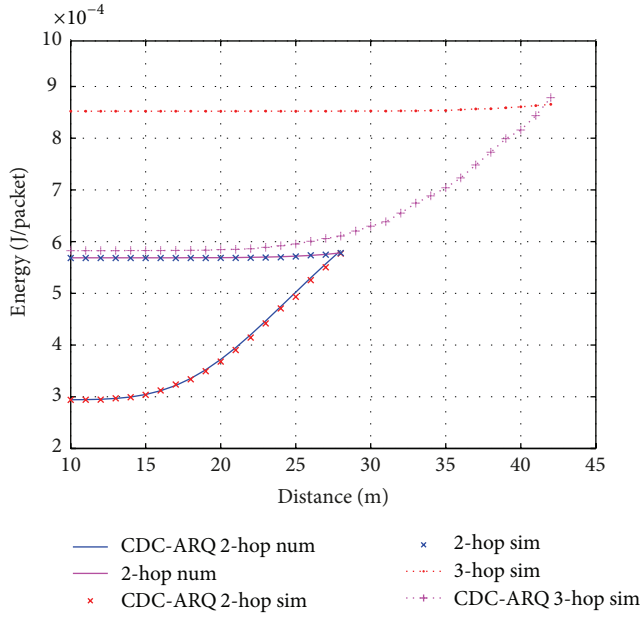

Figure 6: Total mean energy spent per delivered packet with the imposed outage constraint $p_{\text{out}} < 1\%$; multihop and CDC-ARQ forwarding compared.

a smaller σ yields smaller outage probability for $p_{\text{out}} < 0.5$ but provides worse delivery rates for $p_{\text{out}} > 0.5$. Nevertheless, in all studied cases, the direct transmission scheme is inefficient for larger distances and implies the use of either multihop transmission or a CDC-ARQ technique to avoid significant packet loss. We next determine for what distance range one of the three techniques is the most appropriate.

(3) Energy Consumption Optimisation. In the second step, energy consumption is measured in the simulation to verify the model derived in Section 4. While the first step focused on an isolated link, here we study various multinode scenarios. Results show how to optimise system's energy consumption in a multinode scenario. Given the reliability constraints, bounds for optimal link distances are shown to indicate the design choice between direct, multihop, or CDC-ARQ forwarding. For the strict reliability requirement, CDC-ARQ proves to be the most efficient forwarding strategy.

The mean consumed energy per delivered packet of the direct and multihop transmission is compared in Figure 5 for $k = 1$, $k = 2$, and $k = 3$ (the model for E_{eff} in (14) is valid for any k). For $k > 1$ the distance on the graph denotes the total distance traversed from source to destination via relays such that the individual link distance is k times smaller than the total distance. For distances $d < 23$ m there is no need for the multihop transmission because the direct link provides good service while consuming less energy. For $23\,\text{m} < d < 40\,\text{m}$ the optimal setting requires the transmission over two hops, that is, over two equidistant links of $d/2$ meters, past that distance over three hops, and so on. The threshold distance can be obtained numerically from (14) by substituting the corresponding k or from the simulation as Figure 5 shows. The energy consumption significantly increases as the outage probability for the corresponding link distance increases. Namely, packet loss presents a waste of energy resources and has considerable effect on the mean energy consumption. Note in Figure 4 that at distances close to the threshold link distances of $d = 23\,\text{m}$ ($k = 1$) and $d = 20\,\text{m}$ ($k = 2$), even 10–30% of packets can be lost. Therefore, the results presented in Figure 5 apply to systems with loosened reliability requirements but are not suitable for reliability-sensitive systems.

For the applications with strict reliability requirements, link distances must be decreased. In the design phase, maximum p_{out} is fixed in (10) to get the maximum link distance that meets the requirement. For example, when the link outage is set to $p_{\text{out}} < 1\%$, from (10) we get $d = 14\,\text{m}$ as the maximum link distance that still satisfies the outage constraint. Number of hops is next devised depending on the total distance between the source and the destination. In practice this is usually achieved with link estimators that select high-quality and therefore mostly short-range links. The alternative CDC-ARQ technique meets the same reliability requirement with lower energy consumption by including medium-quality links in the communication, besides backup high-quality links. To verify this hypothesis, we study the scenario shown in Figure 1. In this scenario, there is a two-hop path (4-3-2) that can alternate with a medium-quality link (4-2) and a three-hop path (7-6-5-1) that alternates with two medium-quality links (7-5 and 6-1).

Figure 6 shows how much energy can be saved by applying CDC-ARQ in comparison to using the fixed multihop path exclusively. For total distances $14\,\text{m} < d < 28\,\text{m}$ without CDC-ARQ on average 570 μJ of energy is spent per packet on a fixed two-hop path. CDC-ARQ that combines

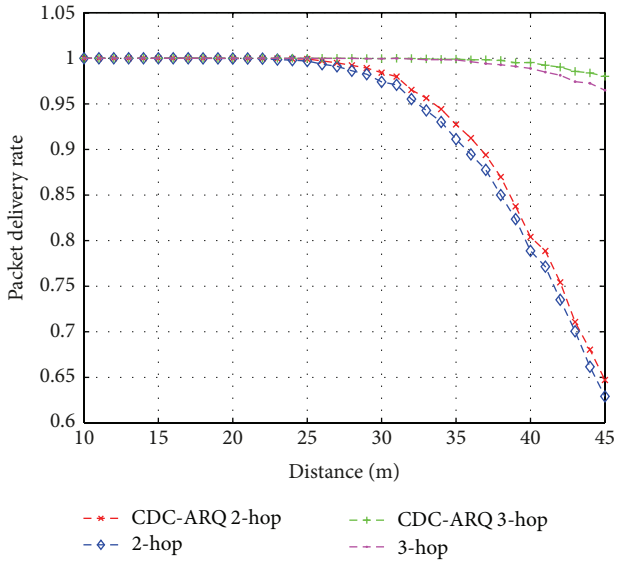

FIGURE 7: Total packet delivery rate for the given source-to-destination distance.

a medium-quality link up to 28 m in length with the two-hop path consumes less energy. The energy savings in CDC-ARQ are obtained when channel conditions allow successful transmissions over a medium-quality link and eventually take less hops to reach the destination. Failures on the medium-quality link represent the cost of the CDC-ARQ. As the link distance increases, there will be more failures and consequently more redirections to the two-hop path. It can be observed that the energy consumption increases accordingly until it becomes equal to the fixed multihop transmission. At the distance $d = 28$ m, about the half of packets are transmitted over a medium-quality link and the other half is redirected. This is a threshold point. Results obtained in simulation agree with the model in (14) and (16).

For source-to-destination distances $28\,\text{m} < d < 42\,\text{m}$, three short-range links are necessary to satisfy the outage constraint. Their mean energy consumption is 850 μJ per delivered packet. When medium-quality links participate in the communication, the energy consumption can again be significantly decreased as Figure 6 shows. Three-hop scenario was verified in simulation only given its analytical complexity. In conclusion, when the reliability demands require multihop transmission over short-range links, CDC-ARQ should be applied to decrease the mean energy consumption per delivered packet.

Although the data packet size L does not influence $\overline{N}_{tx}$ significantly, with the larger L, E_{data} in (5) increases. Consequently, the total energy spent to deliver a packet is larger; for example, $E_{\text{eff}} = 1.24$ mJ when $L = 127$ bytes, $k = 2$, and $p_{\text{out}} < 0.01$ compared to $E_{\text{eff}} = 570\,\mu$J when $L = 27$ bytes. However, apart from the absolute value, the characteristics of energy consumption behaviour for the permitted values of L ($27\,\text{bytes} < L < 127\,\text{bytes}$) closely resemble the ones already commented and shown in Figures 5 and 6.

(4) Packet Delivery Rate. Finally, in order to demonstrate that the presented results satisfy the outage constraint set in advance, the total packet delivery rate for the given source-to-destination distance is measured in the simulation and the results are shown in Figure 7. Just as the model predicts, when $k = 2$ and for the total distances up to $d = 28$ m, the number of discarded packets is limited to less than 1%. The same is confirmed for $k = 3$ and total distances up to $d = 42$ m. The delivery rate decreases for distances greater than the threshold distance obtained from the model such that the reliability requirement cannot be met any more. It can be observed in Figure 7 that CDC-ARQ performs slightly better than the fixed transmission over the multihop path.

6. Conclusion

In this paper, we introduced a metric adequate for low-power wireless links denoted as Average Number of Transmissions per Packet. The metric considers shadow fading and truncated-ARQ. Based on this metric, we were able to calculate the energy consumption of devices compatible with IEEE 802.15.4e, that is, suitable for duty-cycled, low-power, and energy-efficient M2M networks. The energy model presented in this work was validated in the ns-3 network simulator in the realistic simulation environment that mimics the functioning of an actual device. Based on the energy model, we determined the optimal operating regions of direct, multihop, and CDC-ARQ forwarding, as well as the implications of using each. All these results provide useful guidelines on the design of an energy-efficient network, for systems with either loose or strict reliability requirements.

The presented model and the simulation tools can be further refined to include channel hopping and the related channel model implications. Also, more realistic battery models could measure device lifetime. This will be investigated in our future work.

Notations

k:	Number of hops on a multihop path
d:	Link distance in meters
γ:	Instantaneous SNR
$p_s(\gamma)$:	Packet success probability
$p_e(\gamma)$:	Packet error probability
μ:	Mean SNR
σ:	Shadowing standard deviation
$N_{\max}$:	Maximum number of tx attempts per packet
$\overline{N}_{tx}(\mu)$:	Average number of tx per packet
$N_{\text{err}}(\gamma)$:	Number of tx errors
L:	Packet size
p_{out}:	Outage probability when $N_{\max} = 4$
p^c_{out}:	Outage probability when $N_{\text{err}} = 1$
E_{data}:	Energy consumed during data transmission
E_{eff}:	Effective mean energy per delivered packet.

Conflict of Interests

The authors declare that there is no conflict of interests regarding the publication of this paper.

Acknowledgments

This work has been partially funded by the Spanish Government through the research project GEOCOM (TEC2011-27723-C02-01) and by the European Commission under the FP7 Program through the projects NEWCOM# (FP7-318306) and ADVANTAGE (MC-ITN-607774).

References

[1] M. R. Palattella, N. Accettura, X. Vilajosana et al., "Standardized protocol stack for the internet of (important) things," *IEEE Communications Surveys and Tutorials*, vol. 15, no. 3, pp. 1389–1406, 2013.

[2] L. Zhang, R. Ferrero, E. R. Sanchez, and M. Rebaudengo, "Performance analysis of reliable flooding in duty-cycle wireless sensor networks," *Transactions on Emerging Telecommunications Technologies*, vol. 25, no. 2, pp. 183–198, 2014.

[3] IEEE Standard, "Low rate wireless personal area networks (LR-WPANs) amendment 1: MAC sublayer," IEEE Standard 802.15.4e, 2012.

[4] P. Mary, M. Dohler, J.-M. Gorce, G. Villemaud, and M. Arndt, "M-ary symbol error outage over Nakagami-m fading channels in shadowing environments," *IEEE Transactions on Communications*, vol. 57, no. 10, pp. 2876–2879, 2009.

[5] K. Srinivasan, P. Dutta, A. Tavakoli, and P. Levis, "An empirical study of low-power wireless," *ACM Transactions on Sensor Networks*, vol. 6, no. 2, article 16, pp. 1–49, 2010.

[6] M. Dianati, X. Ling, K. Naik, and X. Shen, "Performance analysis of the node cooperative ARQ scheme for wireless ad-hoc networks," in *Proceedings of the IEEE Global Telecommunications Conference (GLOBECOM '05)*, pp. 3063–3067, St. Louis, Mo, USA, December 2005.

[7] T. Predojev, J. Alonso-Zarate, and M. Dohler, "Energy efficiency of cooperative ARQ strategies in low power networks," in *Proceedings of the 31st Annual IEEE Conference on Computer Communications Workshops (IEEE INFOCOM '12)*, pp. 139–144, Orlando, Fla, USA, March 2012.

[8] T. Predojev, J. Alonso-Zarate, and M. Dohler, "Energy evaluation of a cooperative and duty-cycled ARQ scheme for Machine-to-Machine communications with shadowed links," in *Proceedings of the 24th IEEE International Symposium on Personal Indoor and Mobile Radio Communications (PIMRC '13)*, pp. 1640–1644, London, UK, 2013.

[9] Network simulator 3, http://www.nsnam.org/.

[10] J. Deng, Y. S. Han, P.-N. Chen, and P. K. Varshney, "Optimal transmission range for wireless ad hoc networks based on energy efficiency," *IEEE Transactions on Communications*, vol. 55, no. 9, pp. 1772–1782, 2007.

[11] K. Vardhe, C. Zhou, and D. Reynolds, "Energy efficiency analysis of multistage cooperation in sensor networks," in *Proceedings of the 53rd IEEE Global Communications Conference (GLOBECOM '10)*, pp. 1–5, Miami, Fla, USA, December 2010.

[12] G. de Oliveira Brante, M. Kakitani, and R. Souza, "Energy efficiency analysis of some cooperative and non-cooperative transmission schemes in wireless sensor networks," *IEEE Transactions on Communications*, vol. 59, no. 10, pp. 2671–2677, 2011.

[13] J. Alonso-Zarate, L. Alonso, and C. Verikoukis, "Performance analysis of a persistent relay carrier sensing multiple access protocol," *IEEE Transactions on Wireless Communications*, vol. 8, no. 12, pp. 5827–5831, 2009.

[14] M. H. Alizai, O. Landsiedel, J. A. B. Link, S. Gotz, and K. Wehrle, "Bursty traffic over bursty links," in *Proceedings of the 7th ACM Conference on Embedded Networked Sensor Systems (SenSys '09)*, pp. 71–84, Berkeley, Calif, USA, November 2009.

[15] D. Lal, A. Manjeshwar, F. Herrmann, E. Uysal-Biyikoglu, and A. Keshavarzian, "Measurement and characterization of link quality metrics in energy constrained wireless sensor networks," in *Proceedings of the IEEE Global Telecommunications Conference (GLOBECOM '03)*, vol. 1, pp. 446–452, San Francisco, Calif, USA, December 2003.

[16] T. Iwao, K. Yamada, M. Yura et al., "Dynamic data forwarding in wireless mesh networks," in *Proceedings of the IEEE International Conference on Smart Grid Communications (SmartGridComm '10)*, pp. 385–390, Gaithersburg, Md, USA, 2010.

[17] IEEE Standard, "Low rate wireless personal area networks (LR-WPANs)," IEEE Standard 802.15.4, 2011.

[18] M. Z. Zamalloa and B. Krishnamachari, "An analysis of unreliability and asymmetry in low-power wireless links," *ACM Transactions on Sensor Networks*, vol. 3, no. 2, Article ID 1240227, 2007.

[19] N. Baccour, A. Koubaa, L. Mottola et al., "Radio link quality estimation in wireless sensor networks: a survey," *ACM Transactions on Sensor Networks*, vol. 8, no. 4, article 34, 2012.

[20] CC2430 datasheet, 2010, http://www.ti.com/product/CC2430.

[21] Low-rate, wireless personal area network (LR-WPAN) ns-3 model, http://code.nsnam.org/tomh/ns-3-lr-wpan/.